Introducing the IGA approach in plasma physics

Virginie Grandgirard[1], Laura S. Mendoza[2,3], Ahmed Ratnani[2], Eric Sonnendrücker[2,3]

[1]CEA, IRFM, Cadarache, France

[2]Max-Planck-Institut für Plasmaphysik
Garching, Germany

[3]Technische Universität München,
Garching, Germany

3rd International Conference on Isogeometric Analysis, Trondheim, 2015

What is a plasma?

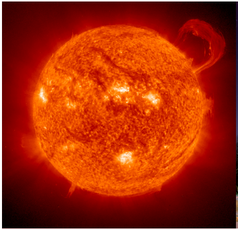

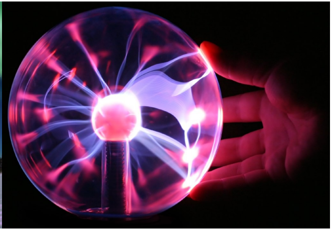

- Plasma is an ionized gas;
- It is known as the fourth state of matter;
- 99% of the mass of the universe is in the plasma state.
- Examples: stars, solar wind, lightning, ...

Controlled fusion and magnetic confinement

D-T Fusion reaction

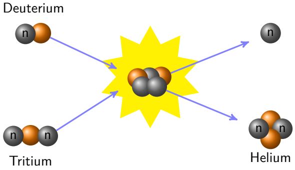

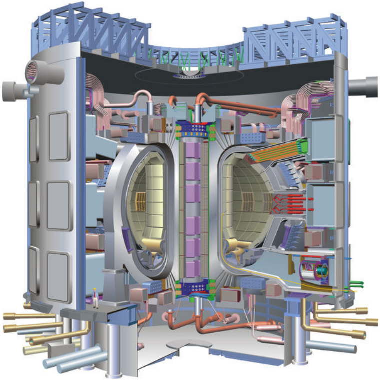

Temperature > 100 Million°K.

⇒ Gas composed of positive ions and negative electrons: plasma

⇒ Plasma responds strongly to electromagnetic fields

⇒ Fusion reactor ITER: controlled fusion by magnetic confinement

Magnetic confinement of a plasma

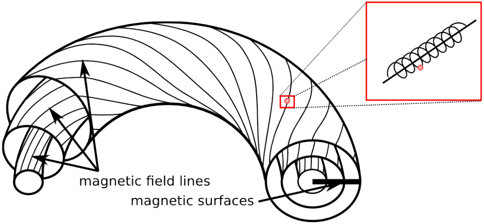

To avoid losses at the ends of the magnetic field, the field lines are usually bent to a torus.

$\longrightarrow$ Need to twist field lines helically to compensate particle drifts.

Motivation: simulating complex plasma shapes

The Gyrokinetic Semi-Lagrangian (**GYSELA**) code:

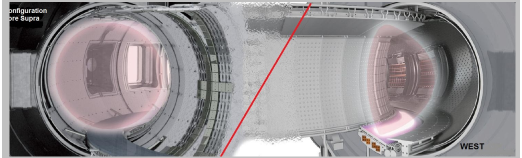

Tore-Supra = circular plasma

WEST = D-shaped plasma

- **Gyrokinetic model**: 5D kinetic (Vlasov) equation on the charged particles distribution + 3D field equation (Maxwell)
- 5 Dimensions: 2 in velocity space, 3 in configuration space
- **Simplified geometry**: concentric toroidal magnetic flux surfaces with circular cross-sections
- Based on the **Semi-Lagrangian** scheme

Motivation: current state of GYSELA's geometry

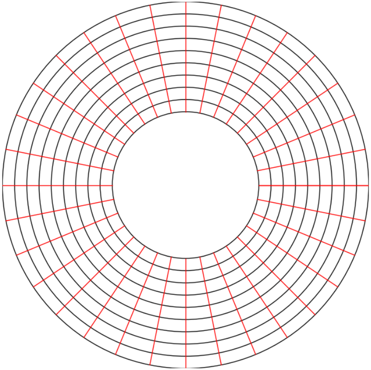

Current representation of the poloidal plane :

- Annular geometry
- **Polar mesh** (r, θ)

Some limitations of this choice :

- Geometric (and numeric) **singular point** at origin of mesh
- Unrepresented area and very costly to minimize that area
- Impossible to represent **complex geometries**

Table of contents

Multi-patch: the general idea

Our original mesh:

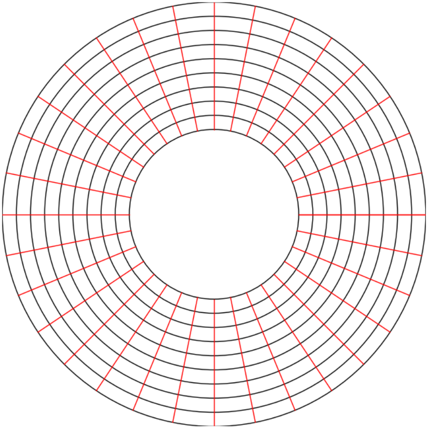

Multi-patch: the general idea

New representation of the poloidal plane:

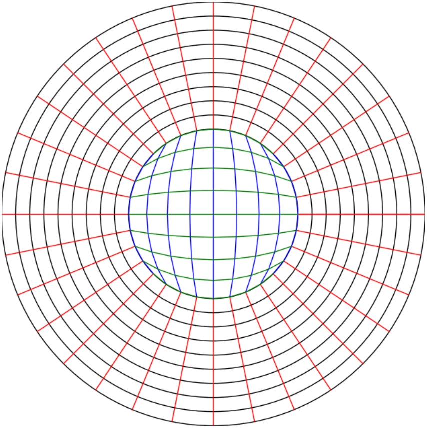

The 5 patches configuration

External crown divided into 4 patches and the connectivity is defined as a patch-edge to patch-edge association (creation tool: **CAID**[1])

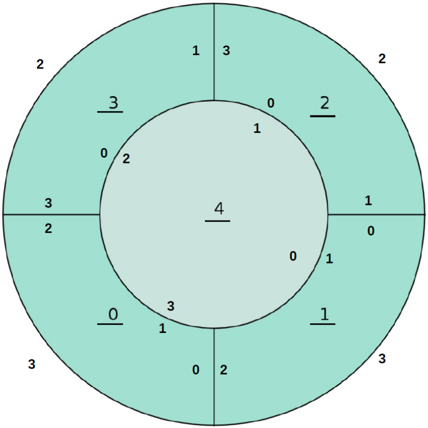

Advantages

- Flexibility defining complex geometries
- Each patch can be treated separately
- No geometrical singularity

New challenges

- What is the best BC?
- How to treat interaction between patches?
- **4 new numerical singularities**

[1] https://github.com/ratnania/caid

Multi-patch: Some results

Results always showed instabilities near singular points. What we've tried to avoid them:

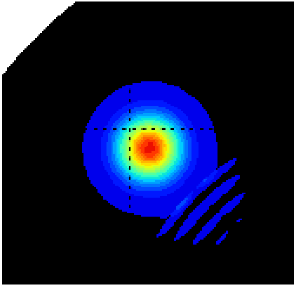

- Boundary conditions tested: strictly interdependent gradients and mean gradients between connecting patches
- Over-lapping: difficulties with interior patch and useless for others
- Squared internal mapping

Problem: Impossible to avoid singular points from mapping from a square to a circle

Possible solution: Stretch the mesh at singular points in order to avoid the singularities

Alternative approach: the hexagonal mesh[2]

Idea: Use a new mapping: **hexagon** $\longrightarrow$ **circle** (*thanks to B.D. Scott and T.T. Ribeiro*).

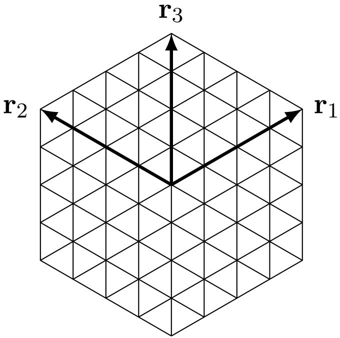

Some advantages:

- No singular points
- (Hopefully) no need for multiple patches for the core of the tokamak
- Twelve-fold symmetry $\Rightarrow$ more efficient programming
- Easy mapping to a disk $\Rightarrow$ field aligned physical mesh

- Regularity of the mesh $\Rightarrow$ easy to find characteristic's feet (BSL)

[2] R. Sadourny, A. Arakawa, and Y. Mintz. "Integration of the nondivergent barotropic vorticity equation with an icosahedral-hexagonal grid for the sphere". *Monthly Weather Review* 6 (1968).

The Backward Semi-Lagrangian Method

We consider the advection equation

$$\frac{\partial f}{\partial t} + \mathbf{a}(x,t) \cdot \nabla_{\mathbf{x}} f = 0 \tag{1}$$

The scheme:

- Fixed grid in phase-space
- Method of characteristics : ODE $\longrightarrow$ origin of characteristics
- Density f is conserved along the characteristics

$$\textit{i.e.} \qquad f^{n+1}(\mathbf{x}_i) = f^n(X(t_n; \mathbf{x}_i, t_{n+1})) \tag{2}$$

- Interpolate on the origin using known values of previous step at mesh points (initial distribution f^0 known).

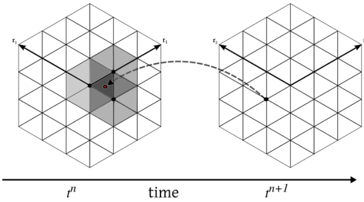

The guiding center model: general algorithm

We consider a reduced model of the gyrokinetic model – a simplified 2D Vlasov equation coupled with Poisson:

$$\begin{cases} \dfrac{\partial f}{\partial t} + E_{\perp} \cdot \nabla_X f = 0 \\ -\Delta \phi = \nabla \cdot E = f \end{cases} \tag{3}$$

The global scheme:

- Known: initial distribution function f^0 and electric field E^0
- For every time step :
  - Solve poisson equation $\Rightarrow E^{n+1}$
  - Apply Semi-Lagrangian method with new electric field $\Rightarrow$ ODE
  - Solve (Leap frog, RK4, ...) ODE to get origin of characteristics $\Rightarrow X^n$
  - Interpolate distribution in $X^n \Rightarrow f^{n+1}$

Two different approaches for interpolation step:
Spline and Hermite Finite Elements interpolations.

Box-splines and quasi-interpolation

Box-Splines:

- Generalization of B-Splines
- Depend on the vectors that define the mesh
- Easy to exploit symmetry of the domain

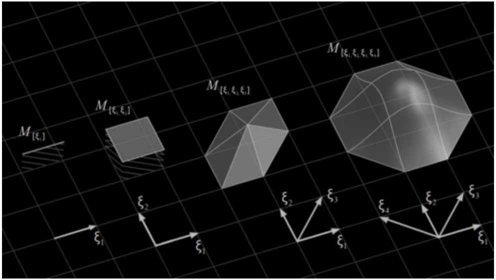

A box-spline $B_M : \mathbb{R}^d \to \mathbb{R}$ associated to the matrix $M = [\xi_1, \xi_2, \ldots, \xi_N]$ is defined, when $N = d$ by

$$B_M(x) = \frac{1}{|detM|}\chi_M(x)$$

else, by recursion

$$B_{M\cup\xi}(x) = \int_0^1 B_M(x - t\,\xi)$$

Box-splines and quasi-interpolation

Box-Spline properties:

- Does not depend on the order of ξ_i in M
- has the support $S = M[0,1)^d$
- is positive on support S
- is symmetric

Quasi-interpolation:

- Distribution function known at mesh points
- Of order L if perfect reconstruction of a polynomial of degree $L-1$
- No exact interpolation at mesh points $f_h(x_i) = f(x_i) + O(\|\Delta x_i\|^L)$

$$f_h(x) = \sum_j c_j B_M(x - x_j) \tag{4}$$

$\Rightarrow$ Additional freedom to choose the coefficients c_j

Main problem: Handling boundary conditions

Non interpolating splines $\longrightarrow$ Problems with Dirichlet boundary conditions

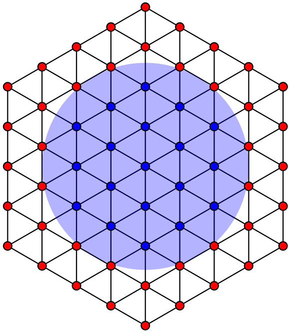

We can differentiate three different types of elements:

- Interior/Exterior elements
- Boundary elements

New questions arise:

- How to derive the equation such that BC intervene?
- Which elements should be considered as interior/exterior?

Nitsche's method[a] $\longrightarrow$ Adding additional terms to weak formulation

[a] A. Embar, J. Dolbow, and I. Harari. *International Journal for Numerical Methods in Engineering* 7 (2010).

Guiding center model : Diocotron instability test case

The Guiding-center model[3]:

$$\begin{cases} \dfrac{\partial f}{\partial t} + E_\perp \cdot \nabla_X f = 0 \\ -\Delta\phi = f \end{cases} \tag{5}$$

with initial distribution function (the diocotron instability in polar coordinates):

$$f(0, r, \theta) = \begin{cases} 1 + \varepsilon\cos(l\cdot\theta), & r^- \leq r \leq r^+ \\ 0, & \text{otherwise} \end{cases} \tag{6}$$

with

- $\varepsilon = 0.1$
- $l = 9.$
- radius $= 10$
- $r^- = 5$ and $r^+ = 8$
- Null Dirichlet boundary condition.

[3] L. S. Mendoza et al. *Solving the guiding-center model on a regular hexagonal mesh*. https://hal.archives-ouvertes.fr/hal-01117196. 2015 (under review).

Comparing results with a FE method

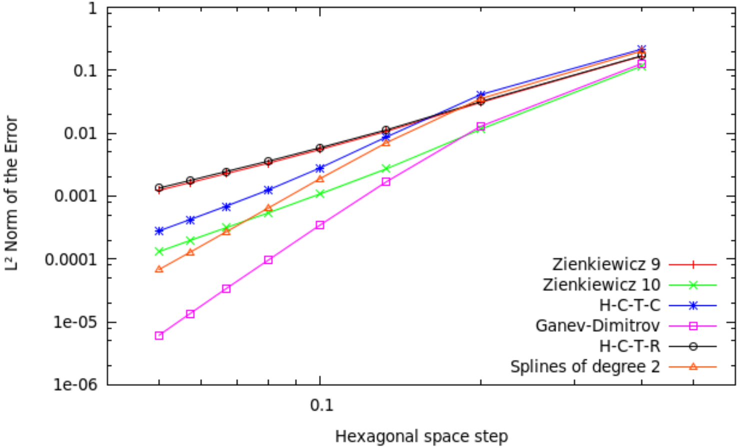

Comparing results with a FE method

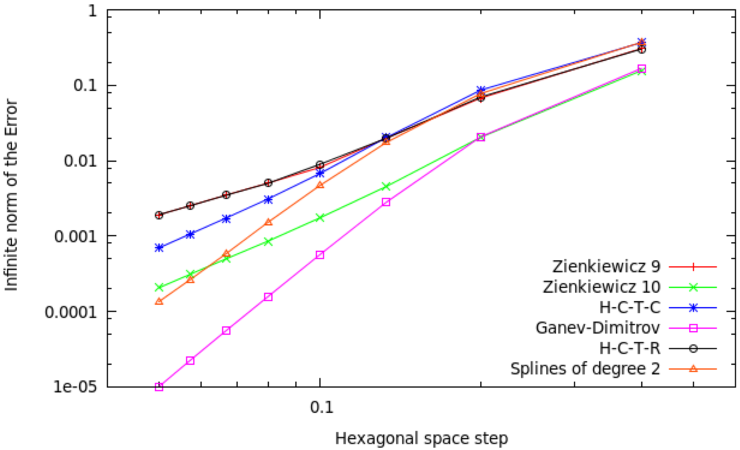

Diocotron instability – Time evolution of the distribution

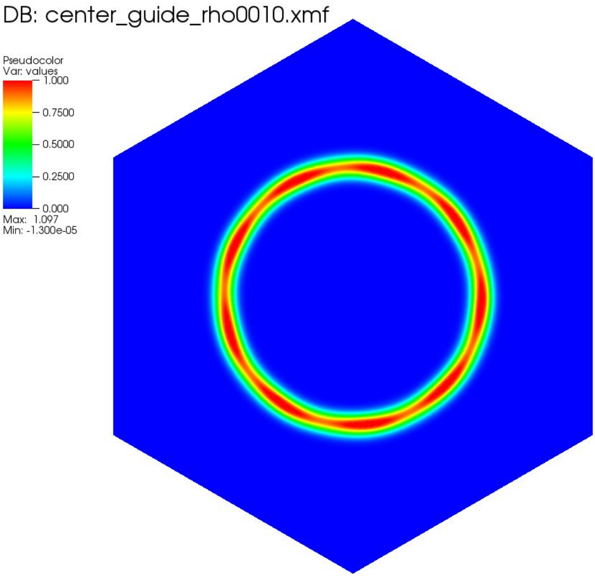

Diocotron instability – Time evolution of the distribution

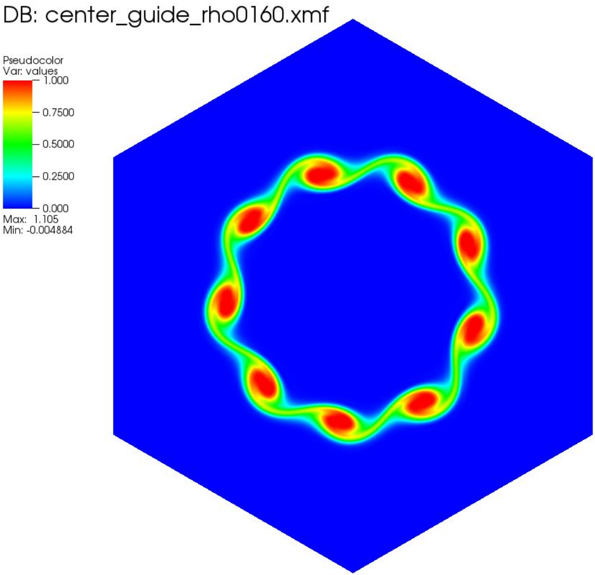

Diocotron instability – Time evolution of the distribution

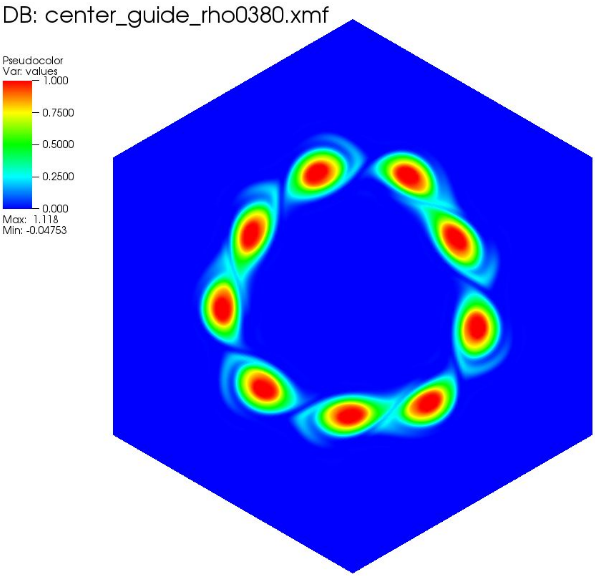

Diocotron instability – Time evolution of the distribution

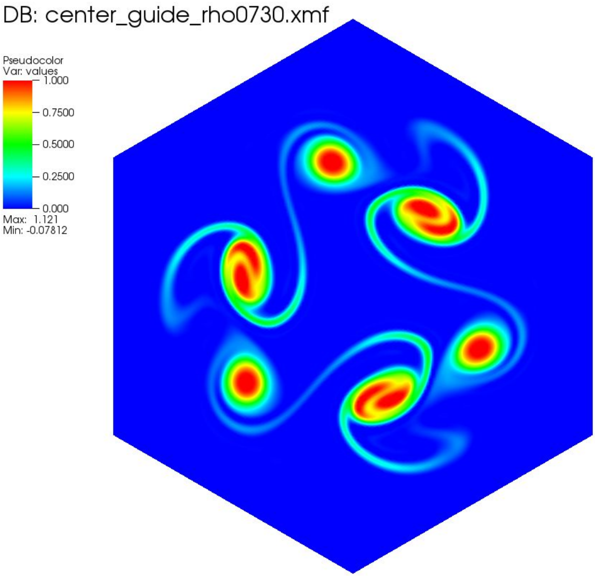

Diocotron instability – Time evolution of the distribution

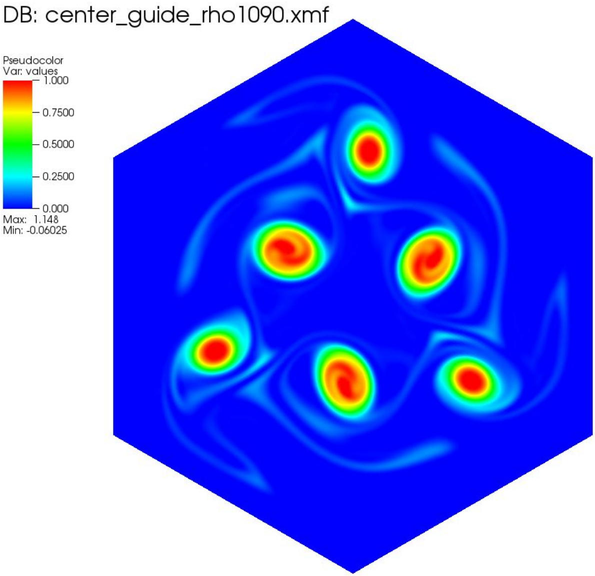

Conclusions and perspectives

Conclusions:

- New mesh with no singular points for modelling the poloidal plane;
- Interpolation scheme adapted to hexagonal meshes:
  - Box-splines adapted to mesh;
  - Quasi-interpolation scheme: efficient scheme.
- Stable method for the Guiding-center model;
- Competitive results (precision/time) with:
  - Multi-patch approach;
  - Hermite Finite Elements method.

Perspectives:

- More complex models to be tested (Vlasov-Poisson, Drift Kinetic, ...);
- IgA with hexagonal mesh as parameter space;
- Implementation of Nitsche's method;
- Other geometry problems: X-point, Scrape-off layer, ...
- Hexagonal mesh for other methods: PIC, ...

Thank you for your attention!

Backup slides

Computing the spline coefficients using pre-filters

Idea: Coefficients obtained by discrete filtering of sample values $f(x_i)$

$$c = p * f = \sum_i f(x_i) p_i \tag{7}$$

prefilters[4]**:** Obtained by solving a linear system of L equations (quasi-interpolation conditions)

Example with $L = 2$:

- We use information on two hexagons from point
- Points at same radius have same weight
- Error: $O(\| \Delta x \|^2)$

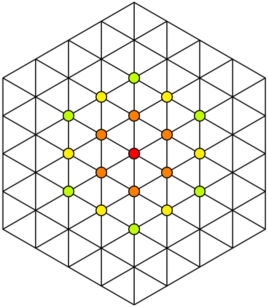

[4] L. Condat, D. Van De Ville, and M. Unser. "Efficient Reconstruction of Hexagonally Sampled Data using Three-Directional Box-Splines." *ICIP*. IEEE, 2006.

Poisson solver : FEM based solver

In cartesian coordinates:

$$\begin{cases} -\Delta_x \phi = f(t,x) & \text{in} \quad \Omega \\ \phi(t,x) = g_d(t,x) & \text{on} \quad \Gamma_{\mathrm{d}} \\ \nabla_x \phi(t,x) \cdot \mathbf{n} = g_n(t,x) & \text{on} \quad \Gamma_{\mathrm{n}} \end{cases}$$

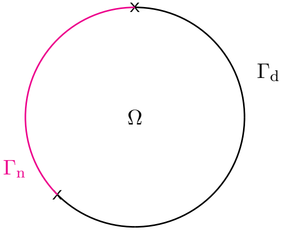

Which we can write in general coordinates such as:

$$-\nabla_\eta \cdot J^{-1}(J^{-1})^T \nabla_\eta \tilde{\phi}(\eta) = \tilde{f}(t,\eta) \tag{8}$$

And its weak formulation

$$-\int_\Omega (\nabla_\eta \tilde{\phi})^T \cdot J^{-1}(J^{-1})^T \nabla_\eta \psi \mid J(\eta) \mid \mathrm{d}\eta = \int_\Omega \tilde{f}(t,\eta)\psi \mid J(\eta) \mid \mathrm{d}\eta \tag{9}$$

with ψ test function, that we will define as a **box-spline**

Poisson solver : Discretization

We discretize the solution ϕ and the test function ψ using the splines (Box- or **B-splines**) denoted B_i as follows

$$\phi^h(\mathbf{x}) = \sum_i \phi_i B_i(\mathbf{x}), \qquad f^h(\mathbf{x}) = \sum_i f_i B_i(\mathbf{x})$$
$$\psi^h(\mathbf{x}) = B_j(\mathbf{x})$$

We obtain

$$\sum_{i,j} \phi_i \left(\int_\Omega \partial_x B_i \partial_x B_j + \int_\Omega \partial_y B_i \partial_y B_j \right) = - \sum_{i,k} f_i \int_\Omega B_i B_k \qquad (10)$$

$\Rightarrow$ **SELALIB**'s general coordinate elliptic solver (developed by A. Back) and **Django** (developed by A. Ratnani et al.) solver

Circular advection test case

A simple but good test is a circular advection model:

$$\partial_t f + y\partial_x f - x\partial_y f = 0 \tag{11}$$

Taking a gaussian pulse as an initial distribution function

$$f^n = \exp\left(-\frac{1}{2}\left(\frac{(x^n - x_c)^2}{\sigma_x^2} + \frac{(y^n - y_c)^2}{\sigma_y^2}\right)\right) \tag{12}$$

Constant CFL ($CFL = 2$) , $\sigma_x = \sigma_y = \frac{1}{2\sqrt{2}}$, hexagonal radius : 8.
Null Dirichlet boundary condition.

Hexagonal mesh: first results

model	Points	a	dt	loops	L_2 error
On mesh points	17101	0.	0.025	1	4.99×10^{-6}
Constant advec.	17101	0.05	0.025	81	4.70×10^{-3}
Circular advec.	17101	1.	0.025	81	4.33×10^{-3}

Box-splines ($deg = 2$) for circular advection:

Cells	dt	loops	L_2 error	L_∞ error	points/μ-seconds
40	0.05	60	3.53E-2	7.74E-2	0.162
80	0.025	120	1.88E-3	4.66E-3	0.162
160	0.0125	240	6.77E-5	1.35E-4	0.162

Dirichlet boundary conditions : Nitsche's method

Using Nitsche's method, we derive the variational form of the Poisson equation which yields[5]:

$$\int_\Omega \nabla\psi\cdot\nabla\phi \mathrm{d}\Omega - \int_{\Gamma d}\psi(\nabla\phi\cdot\mathbf{n})\mathrm{d}\Gamma_d - \int_{\Gamma d}\phi(\nabla\psi\cdot\mathbf{n})\mathrm{d}\Gamma_d + \alpha\int_{\Gamma d}\psi\phi\mathrm{d}\Gamma$$
$$= \int_\Omega \psi f\mathrm{d}\Omega + \int_{\Gamma n}\psi g_n\mathrm{d}\Gamma - \int_{\Gamma d} g_d(\nabla\psi\cdot\mathbf{n})\mathrm{d}\Gamma + \alpha\int_{\Gamma d}\psi g_d\mathrm{d}\Gamma$$

$\Rightarrow$ standard penalty method + additional integrals along Γ_d.

Solutions ϕ respect the boundary condition problem **under some conditions of the stabilization parameter** α

[5] A. Embar, J. Dolbow, and I. Harari. *International Journal for Numerical Methods in Engineering* 7 (2010).

Nitsche's method: coercivity study and the α parameter

We discretize the solution ϕ and the test function ψ using splines like before and we study $rhs(\psi^h, \phi^h)$ at (ψ^h, ψ^h):

$$rhs(\psi^h, \phi^h) = \int_\Omega \nabla\psi^h \cdot \nabla\psi^h \mathrm{d}\Omega - 2\int_{\Gamma d} \psi^h(\nabla\psi^h \cdot \mathbf{n})\mathrm{d}\Gamma_d + \alpha \int_{\Gamma d} (\psi^h)^2 \mathrm{d}\Gamma$$

Using the definition of the L_2-norm : $\| \psi \| = \left(\int_\Omega \psi^2\right)^{1/2}$

$$rhs(\psi^h, \phi^h) = \| \nabla\psi^h \|^2 - 2\int_{\Gamma d} \psi^h(\nabla\psi^h \cdot \mathbf{n})\mathrm{d}\Gamma_d + \alpha \| \psi^h \|^2$$

We define C such that $\| \nabla\psi^h \cdot \mathbf{n} \|^2_{\Gamma d} \leq C \| \nabla\psi^h \|^2$ and using Young's inequality we find that coercivity is ensured when

$$\boldsymbol{\alpha} > \frac{\mathbf{1}}{\mathbf{C(h)}}$$